# PROBING THE WARM GAS IN HIGH REDSHIFT RADIO GALAXIES

*New Results on the Alignment Effect*

MARK J. NEESER, HANS HIPPELEIN AND KLAUS MEISENHEIMER

*Max-Planck-Institut für Astronomie*
*Königstuhl 17, 69117 Heidelberg, Germany*

**Abstract.** We report on the results of an in depth investigation of the extended [O II]$\lambda$3727 line-emission in 11 3CR radio galaxies ($0.5 < z < 1.1$). Using a Fabry-Perot etalon to obtain both the kinematics and morphology of the [O II] gas, our goal was to find the mechanisms responsible for the creation and excitation of this warm gas, and the source of its alignment with the radio emission.

## 1. Introduction

Powerful radio galaxies are often associated with complex extended emission-line regions that can have linear sizes of up to several hundred kpc. The first systematic imaging surveys by Baum et al. (1988) and McCarthy et al. (1987) (low and high z 3CR sources, respectively), and by Chambers et al. (1987) (4C sources) not only revealed a close relationship between the radio power and the optical emission-line luminosity, but also a tendency for the extended gas to share the same axis as that of its double-lobed radio source. Furthermore, the fraction of radio galaxies displaying this emission-line *alignment effect* rapidly changes from a few at low redshifts, to nearly all for $z > 0.3$.

The combination of the novelty of this discovery with the often spectacular morphologies of extended emission-line regions, and their potential effects on the evolution and formation of radio galaxies, attracted lively debate, little consensus, and a large number of possible explanations for this phenomenon. However, since the line-emission regions in high redshift radio galaxies, by virtue of their large intrinsic luminosities and large spatial extents, provide one of the best methods for probing the warm gas at early epochs, the importance of understanding the alignment effect cannot be understated. Since this phenomena arises in extended, highly dynamic gas, an investigation that combines well-resolved morphologies with kinematics would go far in shedding new light on the question of the origin of the warm gas, its source of excitation, its influence on the host galaxy, and the cause of the emission-line/radio source alignment.

## 2. Observational Methods

Selecting the most extended emission-line sources with $z \gtrsim 0.5$ from McCarthy et al. (1995), we imaged a subsample of 3CR radio sources (see table 1) using a Fabry-Perot (FP) interferometer with a spectral and spatial resolution of $\sim$400 kms$^{-1}$ and $\lesssim 1\farcs6$, respectively. By stepping the FP along the [O II]$\lambda$3727 emission-line (typically 8–10 wavelength settings across the line), we were able to simultaneously map the velocity field and morphology of the ionized gas and create a representative sample of 11 radio galaxies observed with unprecedented detail. To investigate the continuum morphologies, as well as subtract their contribution to the line-emission images, intermediate-band ($\lambda/\Delta\lambda \simeq 40$) line-free exposures were also obtained on either side of the redshifted [O II]$\lambda$3727 line.

TABLE 1. Fabry-Perot [O II] Sample

| Source | Redshift | Size of [O II] Region |
|---|---|---|
| 3C 34 | 0.69 | 17" |
| 3C 44 | 0.66 | 10" |
| 3C 54 | 0.83 | 5" |
| 3C 124 | 1.08 | 4" |
| 3C 169.1 | 0.63 | 8" |
| 3C 265 | 0.81 | 35" |
| 3C 337 | 0.64 | 13" |
| 3C 352 | 0.81 | 12" |
| 3C 368 | 1.13 | 9" |
| 3C 435A | 0.47 | 16" |
| 3C 441 | 0.71 | 5" |

## 3. Main Results From the Entire [O II] Sample

Somewhat surprisingly, up to 40% of the radio sources investigated have line-emission regions dominated by the effects of galaxy–galaxy interactions. For these objects we are able to show that the popularly accepted models for exciting the line-emission regions are inadequate to explain all of their observed [O II] features. Instead, we propose a new model in which a close, strong interaction with a companion galaxy exchanges material with the central radio galaxy, creating a complex morphology of bridges, tails and extended knots along the interaction axis. The passage of the companion through the halo of the host source shock heats the supplied gas and the ambient medium, thus creating parts or all of the observed emission-line region and its complex velocity structure. The interaction itself may also be responsible for triggering the radio source of the central galaxy.

Since this new model applies to a significant fraction of the radio source sample, it is important to explain how galaxy–galaxy interactions (an intrinsically geometrically random phenomena) can give rise to alignments between the radio emission and the warm gas. It is plausible that galaxies undergoing gravitational interactions, when aligned with their radio sources, will be preferentially selected by

the flux-limits of the 3CR catalogue. Most models of double radio sources predict that the radio luminosity of a source will be increased if it expands into a denser gaseous medium (see Eales 1992 for a discussion of this effect). Therefore, since only radio galaxies in which one lobe lies near to the line-emission gas supplied by the companion galaxy will experience an enhancement of its radio emission, flux-limited samples will preferentially contain aligned interaction galaxies. The fact that our sources consistently have their brighter and/or closer radio lobe on the same side of the central source as most of its line-emission gas, supports this scenario. Another important clue lies in the fact that all of the interaction galaxies are near to the flux-limit of the 3CR catalogue. This implies that without the radio brightness asymmetries these objects would not have been detected by this survey. By relating the typical radio luminosity and lobe size asymmetries to density differences, we are also able to show that only modest density contrasts ($\frac{\rho_{[\mathrm{OII}]\mathrm{gas}}}{\rho_{\mathrm{IGM}}} \lesssim 7$), between a radio lobe expanding near to the line-emission gas and its counter part expanding into the ambient intergalactic medium on the other side of the central galaxy, are necessary.

For the remaining radio galaxies variations of the more conventional mechanisms—photoionizing radiation from a central, hidden active nucleus, or a direct interaction between the radio source and the ambient medium—are used to explain the excitation and alignment of the [O II]$\lambda$3727 emitting gas. Since each of these three models results in ionized gas morphologies and kinematics that are unique, we are able to use these characteristics to define three distinct classes of line-emission galaxy. The archetype source in each class is shown in bold type.

1. Strong galaxy–galaxy interactions. The sources whose line-emission regions are dominated by this model show one-sided line-emission morphologies distinguished by multiple components, [O II]$\lambda$3727 bridges, and extended linear features. A large range of line-emission sizes and degree of alignment, as well as complex velocity structures are among the features typical of these objects. The intrinsically one-sided nature of the interaction model provides a natural explanation for the very large line-emission brightness, morphology, and velocity asymmetries that define this class (*e.g.* **3C 169.1**, 3C 435A, 3C 44, and the inner region of 3C 265).
2. Photoionization by a central active galaxy, hidden from our view by an obscuring torus. These objects are among the largest and most symmetric sources and are characterized by conical, or bi-conical line-emission structures, and relatively quiescent line widths (*e.g.* **3C 34** and 3C 265).
3. A direct shock interaction between the radio source and the ambient gaseous medium. Galaxies dominated by this model tend to be very well-aligned and have the greatest degree of symmetry in their line-emission luminosity, morphology, and kinematics. They are also characterized by having the largest line widths of all of our sample sources. For a number of galaxies we have also proposed a weaker version of this model, that involves an interaction between the lateral expansion/backflow of the radio lobes and the [O II] gas (*e.g.* **3C 368**, 3C 352, 3C 34, and 3C 337).

The characteristics of each class are sufficiently unique that they can be used

to match a radio galaxy with the mechanisms responsible for the excitation and alignment of its line-emission regions, despite the fact that the line-emission regions of some of our radio galaxies are sufficiently complex that multiple mechanisms for forming and exciting the warm gas are necessary. This fact, together with the three mechanisms needed to explain all of our observations, are a warning against a single, universal model for the alignment effect in all powerful radio galaxies.

Noticeably absent from the list of mechanisms for explaining the emission-line excitation is the popular jet-induced starburst scenario. In this model the radio source propagates through the ambient medium, compresses the gas through its bowshock or overpressure cocoon, and triggers a burst of star formation which is able to *in situ* photoionize the underlying [O II] gas (*e.g.* McCarthy et al. 1987; DeYoung 1989; Begelman & Cioffi 1989). Using the spectral synthesis models of Bruzual & Charlot (1993), we have computed the spectral energy distribution of a starburst constructed to maximize its output of ionizing radiation. Our observed [O II]$\lambda$3727 flux constrains the mass of this burst, allowing a prediction of its continuum signature. Although this computed continuum flux should be easily detectable in our broad-band images, the fact that we find little or no continuum underlying the line-emission components, strongly argues against this model.

## 4. An Example of a High Redshift Photoionization Cone

To give a specific example from the sources discussed in the previous section, we will give a brief description of our results for 3C 34 (z=0.689). A more thorough presentation of this galaxy is given in Neeser et al. (1997). The excitation of the 120 kpc-sized ($H_\circ$=50 km s$^{-1}$ Mpc$^{-1}$, $q_\circ$=0.5) line-emission region of this radio galaxy, is the result of photoionizing radiation emanating anisotropically from a hidden AGN (class 2 emission-line region). This is indicated by the distinctively bi-conical morphology of 3C 34's [O II] gas. By placing the apex of a symmetrical bi-cone at the position of the central continuum source, we find that we can connect 5 distinct line-emission knots/extensions on both sides of the source, and symmetrically straddle the radio source axis (see figure 1).

This model can also explain a number of smaller scale line-emission features: intensity profiles of components that are steepened toward the central source, and components that show various degrees of 'shadowing' outward from the central ionizing source, indicating that the directed UV emission is radiation bounded in parts of the [O II] region. A simple photoionization model shows that this interpretation is energetically viable on these length scales, when the cumulative covering factors of the outermost line-emission components approach unity. The luminosity of the hidden central AGN, necessary to account for the observed [O II]$\lambda$3727 luminosity, is compatible with that of a typical 3CR quasar at a similar redshift.

Although this interpretation can account for the excitation and parts of the warm gas morphology, it is insufficient to explain the observed velocity and linewidth structures. The simplest photoionization model would assume that the ionization cone is merely illuminating the random velocity gas clumps that exist in a typical cluster environment. The difficulties with this interpretation are that the line-emission in 3C 34 is not distributed in discrete clumps, and that the east-

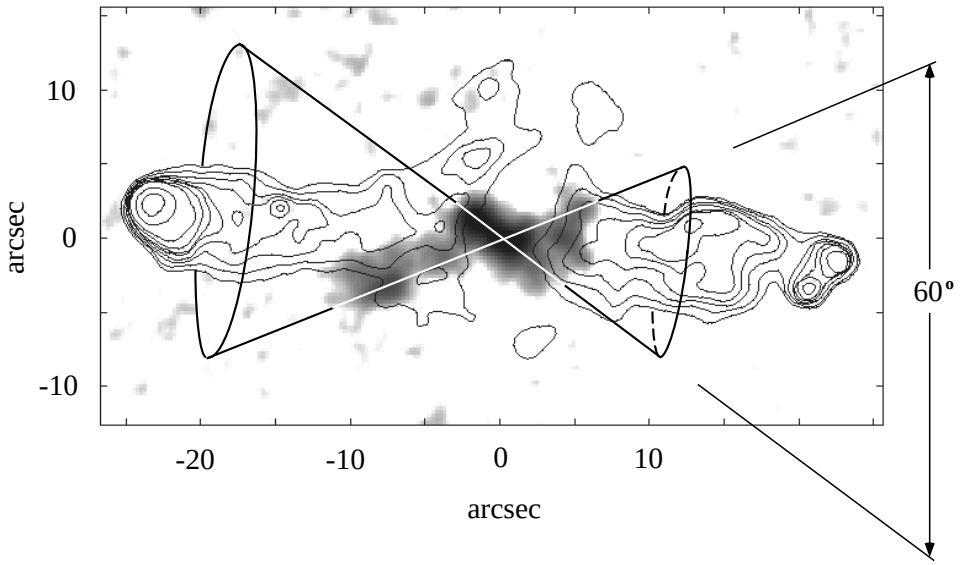


*Figure 1.* Our proposed photoionization cone on the grayscale [O II] image of 3C 34. The 20 cm radio map of Neff et al. (1995) is shown as contours. The apex of the cone is located at the position of the central continuum source (the location of the hidden AGN). An opening angle of 60° is the minimum required to photoionize the observed line-emission.

ern component shows a remarkably flat velocity structure across a length of more than 70 kpc (see figure 2). This indicates that we require a *single* mechanism to act on a large fraction of gas simultaneously. We therefore propose that the radio source has, through the bulk motions of its lateral expansion and backflow, enmasse swept-up the gas that existed in the environment of 3C 34. In this way the gas of the eastern [O II] line-emission region has been compressed, pushed to the outer edge of the radio lobes, and given a bulk velocity that is constant across the entire region. A close correlation between the line-emitting gas and the outer edges of the 20 cm radio emission, as well as the radio depolarization associated with the [O II] gas (Johnson et al. 1995), also support this interpretation.

In our photoionization scenario there exists a direct cause and effect relationship between the radio source and the ionization cone that leads to their alignment in 3C 34. It is possible to imagine that the nucleus was initially surrounded by a cloud opaque to ionizing radiation in all directions. When the radio jet turned on it plowed through the cloud and opened up a low density channel. As the radio lobes grew in size the increased density of the swept-up gas allows it to effectively absorb the incident ionizing radiation from the central AGN; this, in turn, can then effectively escape along the cleared out, low density channel created by the radio source.

The obvious conical structure in 3C 34, though previously unobserved in high redshift, powerful radio galaxies, is well-known in 11 low redshift Seyferts (*e.g.* Wilson & Tsvetanov 1994). The tight alignment between the cone and radio axes found in these sources ($\Delta PA_{mean}$=6°; Wilson & Tsvetanov 1994) is also true for

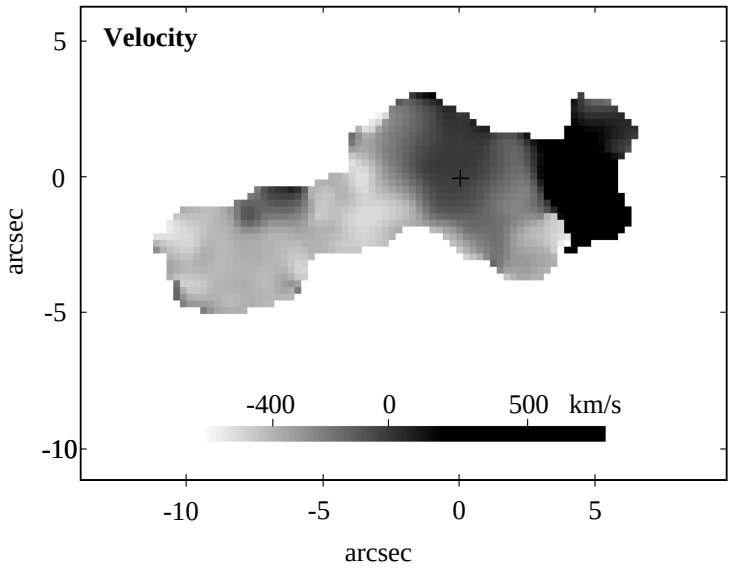


*Figure 2.* A grayscale representation of the radial velocities of the [O II]$\lambda$3727 line-emission in 3C 34. The kinematical and positional origin is defined by the optical continuum counterpart of the radio galaxy (shown with a cross). At the bottom of the image a scale is given matching the diagram's grayscale to velocities in $\mathrm{km\,s^{-1}}$.

3C 34. A fundamental difference, however, is that the Seyfert ionization cones show line-emission gas across the entire lateral extent of their opening angles. The fact that 3C 34's radio power is more than four orders of magnitude greater and hence capable of effectively sweeping out the IGM of the radio galaxy, and confining the line-emitting gas to its edges, is a plausible explanation for this difference.

## References

Begelman, M. C., & Cioffi, D. F. 1989, *Astrophys. J. Lett.*, 345, L21
Bruzual, G. A., & Charlot, S. 1993, *Astrophys. J.*, 405, 538
Chambers, K. C., Miley, G. K., & van Breugel, W. 1987, *Nature*, 329, 604
DeYoung, D. S. 1989, *Astrophys. J. Lett.*, 342, L59
Eales, S. A. 1992,*Astrophys. J.*, 397, 49
Johnson, R. A., Leahy, J. P., & Garrington, S. T. 1995, *Mon. Not. R. Astron. Soc.*, 273, 877
McCarthy, P. J., van Breugel, W., Spinrad, H., & Djorgovski, S. 1987, *Astrophys. J. Lett.*, 321, L29
McCarthy, P. J., Spinrad, H., & van Breugel, W. 1995, *Astrophys. J. Suppl.*, 99, 27
Meisenheimer, K., & Hippelein, H. 1992, *Astron. Astrophys.*, 264, 455
Neeser, M. J., Meisenheimer, K., & Hippelein, H. 1997, *Astrophys. J.*, submitted
Neff, S. G., Roberts, L., and Hutchings, J. B. 1995, *Astrophys. J.*, 99, 349
Wilson, A. S., & Tsvetanov, Z. I. 1994, *Astron. J.*, 107, 1227